PAPER

Check for updates

Potato peel-based PBS/PBAT biocomposites: influence of composition and filler content on injection molded properties

Susanna Miescher, (ID) Florine Schleiffer, Eliane Wegenstein and Selçuk Yildirim (ID) *

The growing demand for sustainable materials has intensified interest in bio-based and biodegradable polymers as alternatives to fossil-based plastics. This study investigated the development of injection-molded biocomposites based on poly(butylene succinate) (PBS), poly(butylene adipate-*co*-terephthalate) (PBAT), and their blends, reinforced with 30–70 wt% potato peels (PP), an abundant by-product of food processing. The effects of filler content and polymer composition on thermal, mechanical, and moisture-related properties were systematically evaluated. All composites remained thermally stable below 228 °C, confirming the suitability of PP for melt processing. FTIR spectroscopy showed no evidence of chemical bonding between filler and polymer matrices, although weak physical interactions were observed, particularly in PBS-rich systems. In contrast, blending PBS with PBAT indicated polymer–polymer interactions, suggesting partial compatibilization, as reflected in a 1.8-fold increase in elongation at break. PP addition consistently altered composite structure and significantly enhanced stiffness, with the elastic modulus increasing from 698 to 1825 MPa for PBS (+162%) and from 77 to 1161 MPa for PBAT (+1418%) at 70 wt% PP. Conversely, tensile strength decreased from 35.0 to 10.6 MPa (PBS) and from 17.1 to 6.5 MPa (PBAT), and elongation at break dropped below 3% for all composites containing ≥40 wt% PP. Overall, PBS/PBAT-potato peel composites exhibited more balanced mechanical performance compared to neat PBS or PBAT composites. DSC analysis revealed that PP acted as a nucleating agent in PBS and PBS-rich blends, increasing crystallization temperature with only minor impact on overall crystallinity. Collectively, these findings demonstrate the feasibility of producing high-filler-content biocomposites for sustainable packaging and agricultural materials.

Sustainability spotlight

In light of the growing demand for sustainable material solutions, this study investigates the use of the biodegradable polymers poly(butylene succinate) (PBS) and poly(butylene adipate-*co*-terephthalate) (PBAT) in combination with an underutilized by-product from the food industry, potato peels (PP). By partially substituting the polymer content with PP, the approach aims to improve resource efficiency, reduce the reliance on virgin polymer input, and create added value from industrial waste streams. This material strategy contributes to the advancement of circular economy principles and aligns with key sustainability targets, including responsible resource use and climate change mitigation as outlined in the United Nations Sustainable Development Goals (SDG 12 and SDG 13).

1 Introduction

Plastics offer numerous functional and economic advantages, but their widespread use has raised growing concerns regarding environmental sustainability.[1,2] With global plastic demand projected to increase, continued reliance on fossil-based polymer systems remains a major challenge. In response, bioplastics have been identified as a promising alternative, with the potential to reduce fossil resource consumption, lower carbon emissions, and support the development of a circular plastics economy.[1,3–6] Research and development in bio-based

and/or biodegradable polymers have gained increasing attention, particularly in the field of aliphatic polyesters such as poly(butylene succinate) (PBS), poly(butylene adipate-*co*-terephthalate) (PBAT), poly(lactic acid) (PLA), poly(ε-caprolactone) (PCL), and polyhydroxyalkanoates (PHAs), among others.[7–10] Due to differences in their physicochemical and mechanical properties, these polymers vary in their suitability for specific applications.[11]

PBS is a biodegradable aliphatic polyester synthesized *via* the polycondensation of succinic acid (or dimethyl succinate) and 1,4-butanediol, combining a relatively low melting temperature of approximately 115 °C with good thermal stability and favorable melt processability.[7,12–14] Its semi-crystalline structure, particularly the degree of crystallinity, influences its mechanical

ZHAW Zurich University of Applied Sciences, Institute of Food and Beverage Innovation, 8820 Waedenswil, Switzerland. E-mail: selcuk.yildirim@zhaw.ch

performance, resulting in moderate stiffness and hardness, with overall properties comparable to those of polypropylene.[13,15] PBAT, on the other hand, is an aliphatic-aromatic polyester synthesized from adipic acid, 1,4-butanediol and terephthalic acid.[16] Due to the aromatic units present in the polymer's structure, PBAT exhibits enhanced toughness and thermal resistance,[17–19] and is characterized by high ductility with greater elongation at break than most other biodegradable polyesters.[16,20]

While both polymers are considered promising materials, their individual limitations restrict their applicability in unmodified form.[9,21] PBS is characterized by low melt viscosity,[12] slow crystallization kinetics,[12] and brittle mechanical behavior,[14,19,22,23] whereas PBAT is primarily limited by its low stiffness and tensile strength.[14] To modify their properties and broaden the range of potential applications, various strategies, such as polymer blending, have been employed to enhance performance and reduce production costs.[24,25] Binary blends of PBS and PBAT, in particular, have gained increasing recognition due to their complementary characteristics. Blending has been reported to result in more balanced mechanical properties, including increased ductility, improved impact strength and toughness,[9,23,26,27] enhanced processability with higher melt flow index (MFI) values,[26] and good polymer compatibility.[26,28] The improved compatibility has been attributed to enhanced interphase interactions, including dipole interactions and hydrogen bonding, which may naturally occur between the two components depending on their relative concentrations.[5,9,21,29]

In addition to polymer blending, the incorporation of various fillers, such as rice husks,[30] lignin,[23] coffee husks,[31] walnut shell powder,[2,24] and starch,[18,19,24] into PBS/PBAT matrices has also been investigated. These fillers not only reinforce the polymer matrix and tailor functional performance of the composites, but also reduce material costs.[23]

Consequently, increasing efforts have been directed toward the use of natural fillers derived from readily available agricultural and food industry by-products. Among these, potato peels have attracted growing interest due to their abundance. With global potato production exceeding 383 million tons annually,[32] and industrial processing continuing to rise, substantial quantities of potato peels are generated as waste streams, amounting to 16–25% of the original crop mass.[33] Potato peels therefore represent a renewable and largely untapped resource with considerable potential for valorization in material-based applications. The peels are composed of starch (16–51%), non-starch polysaccharides (22–27%), including pectin, cellulose, and hemicellulose, as well as lignin (5.8–21.6%), proteins (6–26%), and minerals (6–11.1%).[34–36] Due to this composition and their thermal processability, potato peels have previously been identified as a promising filler material for biocomposite production. The incorporation of 40–60 wt% potato peels into PBS for the production of extruded films has already been investigated.[37] In contrast, injection-molded applications have thus far only been studied with other polymer matrices. Specifically, potato peel powder was incorporated at concentrations of 10–40 wt% into polypropylene[38] and linear low-density polyethylene (LLDPE),[39] each with and without

a compatibilizer, and at a constant concentration of 10 wt% into PLA, with individual formulations prepared using distinct particle size fractions.[40] In all cases, the resulting composites were evaluated with respect to their thermal, mechanical, and physicochemical properties. In all cases, the resulting composites were evaluated with respect to their thermal, mechanical, and physicochemical properties. Although these studies demonstrated the potential of potato peels as a renewable filler capable of increasing material stiffness, they also revealed limitations such as reduced tensile strength and elongation, poor interfacial adhesion, and high moisture sensitivity, primarily due to incompatibility between hydrophilic fillers and hydrophobic matrices.[38,39] These challenges underscore the need for further optimization and tailored formulation strategies.

The use of potato peels as a reinforcing filler in PBS, PBAT, or their blends has so far received limited attention. Therefore, this study investigated the incorporation of potato peels (PP) at concentrations ranging from 30 to 90 wt% into the biopolymers PBS and PBAT. Particular emphasis was placed on assessing the influence of filler content on the thermal, mechanical, and physicochemical properties of the resulting composites. In addition, the effect of polymer composition, including binary blends of the two polymers, on material properties and interfacial compatibility was examined. Evaluating the suitability of this agro-industrial by-product as a filler in biocomposite formulations was intended to promote the development of more sustainable and cost-effective biopolymer systems.

2 Materials and methods

2.1 Materials

Fresh steam-peeled potato peels of the Agria and Fontane varieties were sourced from industrial potato processing (Fresh Food & Beverage Group AG, Bischofszell, Switzerland) and stored at −20 °C until use. Poly(butylene succinate) (PBS; PBI 003, NaturePlast, Mondeville, France) with a density of 1.26 g cm^{-3} and a MFI of 22 g per 10 min (190 °C, 2.16 kg) and poly(butylene adipate-co-terephthalate) (PBAT; Biopolyester purge, BASF SE, Ludwigshafen, Germany) with a density of 1.25–1.29 g cm^{-3} and a MFI of 2.5–4.5 g per 10 min (190 °C, 2.16 kg) were used for composite preparation. Prior to processing, the polymers were dried at 60 °C for approximately 10 h.

2.2 Preparation of potato peel powder

Drying of the thawed potato peels was performed using a vacuum drum dryer (HTC-VTE 140, BHS-Sonthofen GmbH, Herrsching, Germany) at a product temperature of 50 °C and a pressure of 6–10 mbar, followed by post-drying in a drying chamber (FED 260, Binder GmbH, Tuttlingen, Germany) at 45 °C. The dried peels were ground to a particle size below 500 μm using a beater rotor mill (SR 300, Retsch GmbH, Haan, Germany) operating at 3000 rpm. The resulting potato peel powder had a final moisture content of 3.4 ± 0.14% and a starch content of 23.6 ± 2.4%.

2.3 Compounding of biocomposites

The influence of potato peel content on the properties of the neat PBS and PBAT matrices was investigated using a wide filler range of 30–90 wt%, while the effect of PBS/PBAT blending on composite behavior was examined at a fixed filler content of 30 wt%. The composites were compounded according to the formulations shown in Table 1 using a co-rotating twin screw extruder (ZE 18 HMI, Three-Tec GmbH, Seon, Switzerland) equipped with a single-screw feeder (ED 20, Three-Tec GmbH, Seon, Switzerland). Processing was conducted with a screw diameter of 18 mm and a barrel length of 380 mm, at a screw speed of 30 rpm and using a 2 mm nozzle. A consistent temperature profile of 50/100/130/150/150 °C was applied to all formulations. The extruded filaments were subsequently granulated to a size of 4 mm using a pelletizer (DN89-1M ECO, Three-Tec GmbH, Seon, Switzerland).

2.4 Injection molding of potato peel-based specimens

Dog bone test specimens of Type 1BA, conforming to DIN EN ISO 527-2, were produced from the pellets using a laboratory injection molding machine (S/N 21 822, Three-Tec GmbH, Seon, Switzerland). The specimens had a total length of ≥ 75 mm, a width of 5.0 ± 0.5 mm and a thickness of ≥ 2 mm. Injection molding was performed in batches at a melt temperature of 150 °C. An injection pressure of 425 bar was applied for 8 s (increased to 680 bar at 60 wt% PP, 790 bar at 70 wt% PP, and 1415 bar at 80–90% PP), and a holding pressure of 142 N was maintained for 8 s. The mold temperature was set to 60 °C. The injection-molded specimens were conditioned in a climate chamber (VP600, Vötsch Industrietechnik, Balingen, Germany) at 23 °C and 50% RH for at least 24 hours prior to analyses.

2.5 Characterization of sample properties

2.5.1 Fourier transform infrared spectroscopy (ATR-FTIR).
ATR-FTIR spectra of the pure components and of the cross-sections of the injection-molded composites were recorded using a FTIR spectrometer (Frontier, PerkinElmer, USA) in the range of 600–4000 cm^{-1} with a resolution of 4 cm^{-1} and an average of 20 scans.

2.5.2 Thermogravimetric analysis (TGA).
The thermal stability of PP, neat PBS, neat PBAT, and their corresponding composites was evaluated by thermogravimetric analysis (TGA) using a TGA 1/SF system (Mettler Toledo, Greifensee, Switzerland). Approximately 10 mg of samples were placed in an aluminum crucible, and measurements were carried out from 25 °C to 600 °C at a heating rate of 15 °C min^{-1} under a constant nitrogen flow of 40 mL min^{-1}.

2.5.3 Differential scanning calorimetry (DSC).
The thermal properties of the neat polymers, their blends, and all composite formulations were analyzed by differential scanning calorimetry (DSC) on pelletized samples. Approximately 7 ± 0.5 mg of each sample was placed in a Tzero aluminum hermetic pan with a pierced lid and subjected to a heating–cooling–heating cycle under a nitrogen atmosphere. The temperature program ranged from −90 to 250 °C with heating and cooling rates of 10 °C min^{-1}, including isothermal holds of 1 min at 250 °C and 5 min at −90 °C (DSC Q2000, TA Instruments, Waters GmbH, Eschborn, Germany). The crystallization temperature (T_c) and crystallization enthalpy (ΔH_c) werde derived from the cooling run, while the glass transition temperature (T_g), cold crystallization temperature (T_{cc}), cold crystallization enthalpy (ΔH_{cc}), melting temperature (T_m), and melting enthalpy (ΔH_m) werde determined from the second heating run. The degree of crystallinity (X_c) was calculated using eqn (1):

Table 1 Composition of PBS, PBAT, their blends, and the corresponding composites containing potato peels (PP)

Polymer matrix	Sample	PBS [wt%]	PBAT [wt%]	PP [wt%]
PBS	PBS	100		
	PBS 70_PP 30	70		30
	PBS 60_PP 40	60		40
	PBS 50_PP 50	50		50
	PBS 40_PP 60	40		60
	PBS 30_PP 70	30		70
	PBS 20_PP 80	20		80
PBAT	PBAT		100	
	PBAT 70_PP 30		70	30
	PBAT 60_PP 40		60	40
	PBAT 50_PP 50		50	50
	PBAT 40_PP 60		40	60
	PBAT 30_PP 70		30	70
	PBAT 10_PP 90		10	90
PBS/PBAT	PBS 70/PBAT 30	70	30	
	PBS 50/PBAT 50	50	50	
	PBS 30/PBAT 70	30	70	
	(PBS 70/PBAT 30) 70_PP 30	49	21	30
	(PBS 50/PBAT 50) 70_PP 30	35	35	30
	(PBS 30/PBAT 70) 70_PP 30	21	49	30

$$X_c = \left[\frac{\Delta H_m - \Delta H_{cc}}{f \times \Delta H_{m100\%}} \right] \times 100 \qquad (1)$$

where ΔH_m is the melting enthalpy, ΔH_{cc} is the cold crystallization enthalpy, f is the weight fraction of PBS, PBAT or PBS/PBAT blends in the composite, and $\Delta H_{m100\%}$ is the theoretical melting enthalpy of 100% crystalline polymer, taken as 200 J g^{-1} for PBS[41,42] and 114 J g^{-1} for PBAT.[14]

2.5.4 Mechanical properties. The mechanical properties of the dog bone test specimens were evaluated by tensile and flexural testing, with eight replicates performed per material. Tensile properties, including tensile modulus E_t [MPa], tensile strength σ_m [MPa] and elongation at break ε_b [%] were determined according to DIN EN ISO 527-2 using a material testing machine (ProLine Z005 TH, ZwickRoell GmbH & Co. KG, Ulm, Germany) equipped with a 5 kN load cell, pneumatic grips rated to 2.5 kN, and an extensometer with a gauge length of 25 mm. A clamping length of 60 mm was used, with a test speed of 1 mm min^{-1} for the determination of tensile modulus and 50 mm min^{-1} for the determination of yield stress. Flexural properties, specifically flexural modulus E_f [MPa] and flexural strength σ_{fM} [MPa], were measured in accordance with DIN EN ISO 178 using a three-point bending test using a material testing machine (Zwicki Z0.5 TH, ZwickRoell GmbH & Co. KG, Ulm, Germany) equipped with a 500 N load cell and a support span of 64 mm. The crosshead speed was set to 50 mm min^{-1}.

2.5.5 Water contact angle (WCA). The wetting behavior of the sample surfaces was evaluated by static water contact angle (WCA) measurements using the sessile drop method. Measurements were carried out using a goniometer (OCA15pro, DataPhysics Instruments GmbH, Filderstadt, Germany), equipped with automated image acquisition software (Dataphysics SCA20). A 10 µl droplet of ultrapure water was dispensed onto the surface of each of five replicate specimens, and the contact angle was determined using the Young–Laplace fitting method.

2.5.6 Water uptake capacity (WUC). The water uptake capacity of the biocomposites was determined according to EN ISO 62:2008, with a deviation from the standard by using complete dog bone specimens. The samples were dried in a drying chamber (FED 260, Binder GmbH, Tuttlingen, Germany) at 50 °C for 24 h to determine the initial dry weight (m_1). Subsequently, the specimens were fully immersed in 300 mL of distilled water at 23 °C, and the wet weight (m_2) was recorded after 24 h, following gentle blotting of surface water with filter paper. The final dry weight (m_3) was determined after re-drying at 50 °C for more than 24 h. All measurements were performed in five replicates. Water uptake capacity (WUC) and soluble matter loss (SML) were calculated using eqn (2) and (3).

$$\text{WUC}(\%) = \frac{m_2 - m_3}{m_1} \times 100 \qquad (2)$$

$$\text{SML}(\%) = \frac{m_1 - m_3}{m_1} \times 100 \qquad (3)$$

2.5.7 Statistical analysis. Statistical evaluation was performed for data on mechanical properties, water contact angle,

and water uptake capacity. Results are presented as mean ± standard deviation. Data were tested for normality using the Shapiro–Wilk test and for homogeneity of variances using Levene's test. If both assumptions were met, a one-way analysis of variance (ANOVA) followed by Tukey's HSD *post hoc* test was conducted. If at least one assumption was violated, the non-parametric Kruskal–Wallis test followed by the Conover–Iman *post hoc* test was applied. A *p*-value < 0.05 was considered statistically significant.

3 Results & discussion

Potato peels (PP) were incorporated into PBS, PBAT, and their blends at loadings ranging from 30 to 90 wt%. While compounding was technically feasible across this range, formulations containing 80–90 wt% filler exhibited pronounced brittleness, which compromised their processability and hindered further fabrication into injection-molded specimens. Consequently, only formulations containing up to 70 wt% PP were considered for subsequent analyses. The injection-molded dog bone specimens of the various composite formulations are presented in Fig. 1. The incorporation of PP resulted in a pronounced brown coloration, irrespective of the polymer matrix, with slightly increased intensity at higher filler contents. Additionally, specimens with elevated filler loadings exhibited a fibrous texture and visible inhomogeneities.

3.1 Fourier transform infrared spectroscopy (ATR-FTIR)

The chemical composition of PBS, PBAT, potato peels, and the corresponding composite materials was analyzed by Fourier-transform infrared (FTIR) spectroscopy. The spectra of neat PBS and PBAT (Fig. 2a) exhibited characteristic absorption bands representative of the respective polymers. Peaks at 2946/2955, 1711/1713, and 1149/1163 cm^{-1} were assigned to the asymmetric stretching of C–H groups, the C=O stretching of carbonyl groups within polyester structures, and the C–O–C stretching vibrations of ester linkages, respectively.[14,43,44] In the carbonyl stretching region between 1700 and 1740 cm^{-1}, however, a distinction between crystalline and amorphous regions in the semicrystalline polymers[14,43] could only be identified by a weak shoulder (~1727 cm^{-1}) due to overlapping signals. The weak absorptions observed around 3400 cm^{-1} may be attributed to hydroxyl-containing species, including chain-end functionalities and residual moisture.[14,43,45] Additionally, the out-of-plane bending vibration of aromatic C–H bonds at 726 cm^{-1} in PBAT confirmed the presence of phenylene rings.[14,43]

The blends exhibited a more complex pattern of carbonyl group vibrations, including a shift of the peak mainly in PBS 70/PBAT 30 to 1717 cm^{-1}, which may indicate interactions between the polyester chains. This effect has been previously interpreted as evidence of a chemical reaction, such as the formation of PBS-PBAT copolyesters through ester–ester interchange reactions, which may serve as a compatibilizer within the system.[9,29,43,46] However, the extent of this transesterification was reported to decrease with increasing PBAT content.[9]
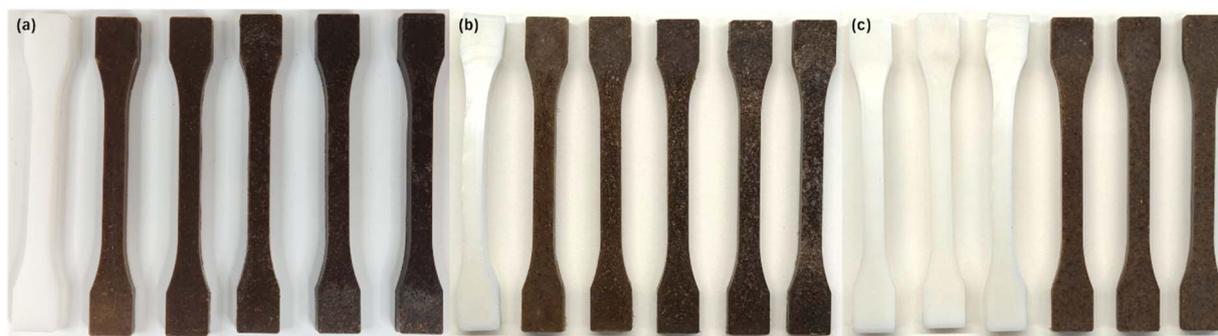
Fig. 1 Injection-molded dog bone specimens of (a) PBS and its composites containing 30, 40, 50, 60, and 70 wt% potato peels (PP); (b) PBAT and its composites with 30, 40, 50, 60, and 70 wt% PP; and (c) PBS/PBAT blends with mass ratios of 70/30, 50/50, and 30/70, each containing 30 wt% PP.

Potato peels, characterized by a complex composition of starch, cellulose, hemicellulose, lignin, and protein, displayed a broad range of overlapping absorption bands in the FTIR spectrum (Fig. 2b), assignable to various functional groups. The broad band observed between 3600–3000 cm^{-1} resulted from overlapping O–H stretching vibrations, primarily originating from carbohydrates such as cellulose and starch,[36,47,48] as well as N–H stretching vibrations associated with proteins.[36] A distinct peak at 2919 cm^{-1} was attributed to C–H stretching of methyl and methylene groups,[36,47,48] as typically found in lipids, lignin, and polysaccharides. Peaks in the region of 1600–1400 cm^{-1} were associated with C=C stretching vibrations of aromatic rings attributed to lignin,[36] as well as C=O stretching vibrations related to protein content.[36,47] Furthermore, the band at 1240 cm^{-1} was tentatively assigned to C–O–C stretching, likely linked to the presence of lipids and suberin in potato peels.[36] The strong and broad absorption around 1020 cm^{-1} was attributed to C–O–C vibrations of pyranose sugar rings and is characteristic of polysaccharide-rich matrices.[36,48]

The incorporation of PP did not alter the spectral profiles, indicating that no chemical interactions occurred between the filler and the polymer matrices. Therefore, of the polymer blends investigated, only the compound PBS 70/PBAT 30 is included in Fig. 2b as a representative example. However, minor peak shifts and changes in intensity, particularly upon incorporation into PBS, may suggest weak physical interactions, such as hydrogen bonding,[49] or slight alterations in filler dispersion or crystallinity. The observation that filler and matrix largely remain chemically distinct has also been reported for the incorporation of PP into PLA[40] and for the use of starch in PBS and PBAT.[18,50]

3.2 Thermal properties

3.2.1 Thermogravimetric analysis (TGA). The thermal stability of PBS, PBAT, and their blends, as well as the effects of potato peel incorporation, were evaluated using thermogravimetric analysis (TGA). The corresponding decomposition behaviors are shown in Fig. 3, including derivative
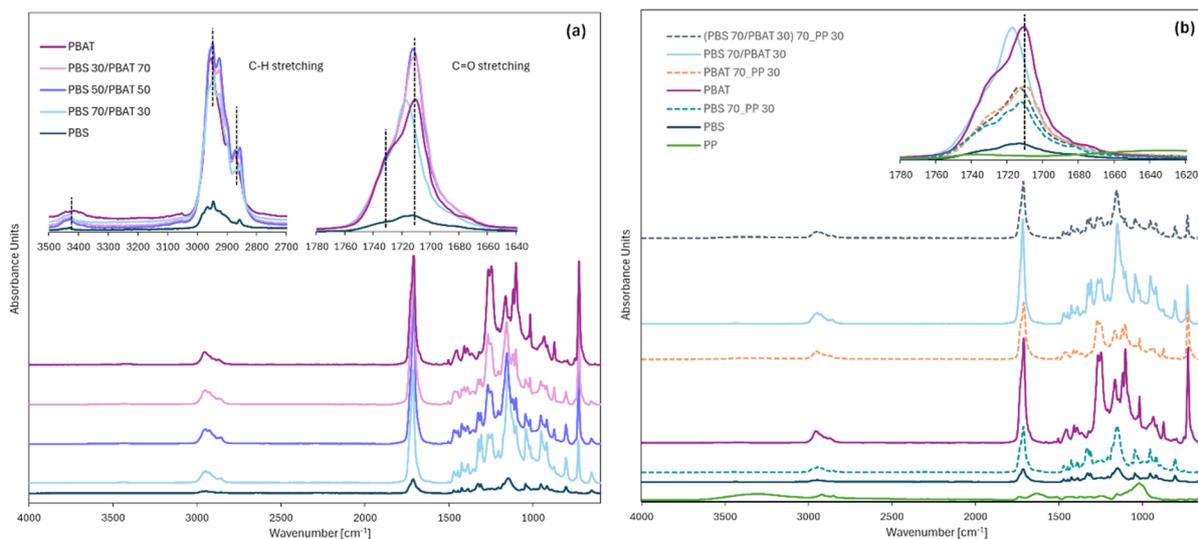

Fig. 2 FTIR absorption spectra of (a) neat PBS, PBAT and their blends, and (b) potato peels (PP) and its composites with PBS, PBAT and the blend PBS 70/PBAT 30 at 30 wt% PP content, measured in the range of 600–4000 cm^{-1}.
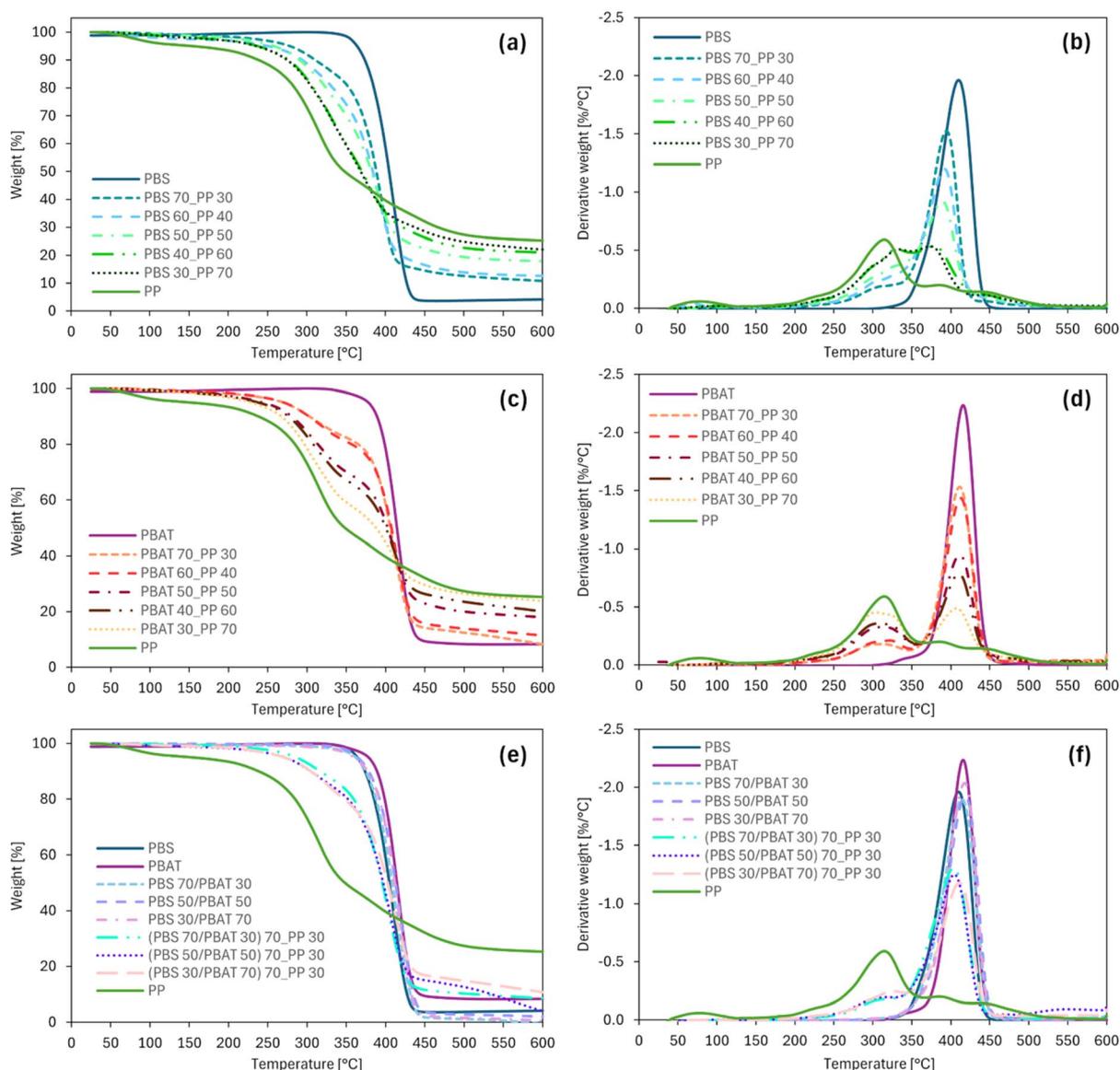
Fig. 3 TGA (a) and DTG curves (b) of PBS and its composites containing 30–60 wt% potato peels (PP), TGA (c) and DTG curves (d) of PBAT and its composites containing 30–60 wt% PP, and TGA (e) and DTG curves (f) of PBS/PBAT blends and its composites containing 30 wt% PP.

thermogravimetry (DTG) curves for enhanced interpretation of the degradation steps; key TGA parameters are summarized in Table S1 (SI). The neat polymers exhibited a single-step degradation, with maximum decomposition rates observed at 409.5 °C for PBS and 415.75 °C for PBAT. The onset of thermal degradation indicated a slightly higher thermal stability for PBAT compared to PBS, consistent with literature data.[5,9,14] Due to the similar degradation profiles of PBS and PBAT, their blends likewise exhibited single-step degradation profiles, with the peak degradation temperature shifting according to the respective polymer ratios. Accordingly, and in agreement with previous findings, melt blending did not adversely affect the thermal stability of the polymers.[5,9]

In contrast, potato peels exhibited a multi-step degradation profile comprising four distinct stages. The peak observed around 78 °C is commonly attributed to the evaporation of moisture and other volatile compounds.[38,51] The most prominent decomposition event, with a maximum at 314.5 °C, corresponds to the thermal degradation of polysaccharides, including starch (280–350 °C),[36,51] cellulose (275–400 °C),[25,36,51] hemicellulose (220–315 °C)[36] and pectin (150–350°).[25] Additional minor peaks at 385 °C and 438 °C are associated with the degradation of more thermally stable constituents such as lignin and suberin (250–500 °C)[25,36] Furthermore, the degradation of lipids and proteins occurs across the entire temperature range (200–600 °C),[25] contributing to the broad and overlapping degradation profile.

The incorporation of potato peels into PBS and PBAT led to a progressive reduction in thermal stability in both polymer systems, directly correlated with filler concentration, as

evidenced by the shift in $T_{5\%}$ values, from 364.00 to 235.50 °C for PBS and from 378.25 to 228.75 °C for PBAT, observed at 70 wt% PP content. With increasing filler loading, the degradation profiles of the biocomposites gradually transitioned toward that of PP itself. In parallel, the residue content increased from 4.13 to 22.08% for PBS and 8.32 to 23.78% for PBAT at 600 °C with 70 wt% filler loading, reflecting the presence of higher amounts of thermally stable inorganic or ash-forming components derived from the potato peels. A similar trend was already reported by Sugumaran *et al.* (2015)[38] for the incorporation of potato peels into polypropylene. Comparable changes in thermal stability were observed in the PBS/PBAT blends upon addition of potato peels, including a shift toward lower degradation temperatures and the emergence of a multi-step degradation profile, attributable to the higher filler content. Overall, the reduced thermal stability of the composites necessitates processing at temperatures below 228 °C. However, this remains feasible given the relatively low melting and processing temperatures of PBS and PBAT, and the resulting biocomposites remained thermally stable under the applied conditions.

3.2.2 Differential scanning calorimetry (DSC). To investigate the thermal behavior of PBS, PBAT, and their blends, as well as the effects of potato peel incorporation, DSC was employed to determine the crystallization temperature (T_c), crystallization enthalpy (ΔH_c), glass transition temperature (T_g), cold crystallization temperature (T_{cc}), cold crystallization enthalpy (ΔH_{cc}), melting temperature (T_m), melting enthalpy (ΔH_m), and the degree of crystallinity (X_c) of the polymer phase (Table 2).

The neat polymers each exhibited characteristic crystallization and melting behaviors. PBS showed a crystallization temperature of 66.89 °C, a cold-crystallization peak at 97.34 °C, and a distinct melting peak at 115.01 °C, all of which are consistent with its semicrystalline nature. In contrast, PBAT, due to its predominantly amorphous character, displayed a lower crystallization temperature of 43.47 °C, along with a broad and weak melting area centered around 121.83 °C, without evidence of cold crystallization. The incorporation of potato peels led to altered, yet distinct, thermal behavior in both polymer systems. In the case of PBS, filler addition resulted in a pronounced increase in crystallization temperature to approximately 83 °C, irrespective of its concentration. Simultaneously, the crystallization enthalpy, normalized to the polymer content, increased proportionally with PP loading. This observation aligns with previous findings indicating that dispersed filler particles at low concentrations can act as heterogeneous nucleation sites, thereby promoting crystallization within the polymer matrix.[2,52] In the present study, this nucleating effect was still evident at a filler content of 70 wt%. The increased degree of primary crystallization upon cooling, accompanied by a concurrent reduction in cold crystallization, suggests a rearrangement within the crystallization process, however, the overall degree of crystallinity of the PBS-PP composites showed only a moderate increase at intermediate filler loadings, with the effect plateauing or even declining at higher concentrations.

In the case of PBAT, the incorporation of potato peels led to an even more pronounced shift in crystallization toward higher temperatures, reaching 85.55 °C at 30 wt% PP with a minor drop to 75.37 °C observed at 70 wt% PP. Simultaneously, however, a reduction in the crystallization enthalpy was observed. This suggests that while PP promoted nucleation, the extent of crystallization was limited, possibly due to restricted chain

Table 2 Thermal properties of PBS, PBAT and PBS/PBAT blends, as well as their corresponding composites containing 30−70% potato peels (PP). Shown are the glass transition temperature (T_g), crystallization temperature (T_c), crystallization enthalpy (ΔH_c), cold crystallization temperature (T_{cc}), cold crystallization enthalpy (ΔH_{cc}), melting temperature (T_m), melting enthalpy (ΔH_m), and degree of crystallinity of the polymer phase (X_c). Values in parentheses are normalized to the polymer or polymer blend content

Polymer matrix	Sample	T_g [°C]	T_c [°C]	ΔH_c [J g^{-1}]	T_{cc} [°C]	ΔH_{cc} [J g^{-1}]	T_m [°C]	ΔH_m [J g^{-1}]	X_c
PBS	PBS	−29.38	66.89	58.41	97.34	9.09	115.01	63.26	27.09
	PBS 70_PP 30	−25.81	83.32	47.94 (68.49)	103.12	4.98 (7.11)	114.88	45.30 (64.71)	28.80
	PBS 60_PP 40	−26.45	83.36	43.57 (72.62)	104.50	3.50 (5.83)	115.24	41.21 (68.68)	31.43
	PBS 50_PP 50	−22.79	83.49	29.58 (59.16)	105.21	1.51 (3.02)	116.88	28.15 (56.30)	26.64
	PBS 40_PP 60	−18.46	83.58	27.85 (69.63)	105.50	1.62 (4.05)	117.10	25.96 (64.90)	30.43
	PBS 30_PP 70	−22.70	83.22	19.29 (64.30)	106.08	0.98 (3.28)	117.43	18.52 (61.73)	29.23
PBAT	PBAT	−25.85	43.47	16.70	—	—	121.83	5.90	5.18
	PBAT 70_PP 30	−33.10	85.55	5.39 (7.70)	—	—	124.98	1.86 (2.66)	2.33
	PBAT 60_PP 40	−25.81	76.75	2.12 (3.53)	—	—	125.29	1.13 (1.89)	1.66
	PBAT 50_PP 50	−28.91	77.18	4.97 (9.93)	—	—	125.19	1.79 (3.59)	3.15
	PBAT 40_PP 60	−27.40	76.47	2.76 (6.89)	—	—	126.55	0.91 (2.28)	2.00
	PBAT 30_PP 70	−26.19	75.37	0.90 (2.99)	—	—	126.48	0.75 (2.49)	2.19
PBS/PBAT	PBS	−29.38	66.89	58.41	97.34	9.09	115.01	63.26	—
	PBAT	−25.85	43.47	16.70	—	—	121.83	5.90	—
	PBS 70/PBAT 30	−28.78	69.46	45.50	97.67	—	114.92	45.48	—
	PBS 50/PBAT 50	−31.11	63.43	27.67	98.30	—	113.55	27.74	—
	PBS 30/PBAT 70	−32.71	50.23	7.44	—	—	113.04	0.78	—
	(PBS 70/PBAT 30) 70_PP 30	−36.22	71.22	36.44 (52.06)	96.46	6.70	112.84	37.38 (53.40)	—
	(PBS 50/PBAT 50) 70_PP 30	−35.58	69.06	26.64 (38.06)	97.29	4.15	112.84	25.30 (36.14)	—
	(PBS 30/PBAT 70) 70_PP 30	−31.32	72.38	16.74 (23.91)	95.96	4.05	114.50	17.24 (24.63)	—

mobility and reduced crystalline order. It has already been reported in the literature that filler incorporation may reduce crystal growth and crystallization rates by hindering polymer chain mobility.[2,19,53] Pivsa-Art et al. (2016) further demonstrated that the influence of a filler is not uniform across different polymer systems; for instance, talc enhanced the crystallization of PLA while simultaneously suppressing the crystallinity of PBS.[54] In the present study, inhibition of crystallization was supported by a marked decrease in melting enthalpy, from 5.90 to 2.49 J g^{-1}, and a corresponding reduction in X_c.

In the blends, the thermal properties of the two polymers appeared to be superimposed, with the respective behavior largely dominated by the polymer present in higher proportion (Fig. 4a and b). The crystallization temperature shifted toward an intermediate value between the neat polymers, exhibiting a bimodal peak, particularly pronounced in the PBS 70/PBAT 30 formulation. In contrast to the findings of de Matos Costa et al. (2020), however, a distinct PBS-associated peak component was observed in this system, exhibiting greater intensity than in neat PBS.[14] A previous study already demonstrated that the crystallization of PBS can be promoted in the presence of PBAT, possibly due to molecular interactions such as hydrogen bonding.[52] In the present study, crystallization was predominantly governed by the PBS component, except in the PBS 30/PBAT 70 blend, suggesting that PBAT may act as a nucleating agent for the PBS phase. At higher PBAT contents, PBS crystallization appeared to be inhibited, consistent with findings reported by Nobile et al. (2018).[55] This inhibitory effect was further evidenced by the progressive decrease in cold crystallization and melting enthalpies with increasing PBAT content. A reliable

determination of the degree of crystallinity was, however, not feasible due to the overlapping peaks of PBS and PBAT. Furthermore, the PBS-dominated crystallization behavior would have skewed the values normalized to PBAT, resulting in inaccurate representations of its individual contribution. Potato peel addition (Fig. 4c and d) intensified the PBS-dominated crystallization, resulting in elevated crystallization temperatures and increased crystallization enthalpy, similar to the behavior observed in the neat polymers, with both effects attributable to the filler acting as a nucleating agent.[2,52,53] Simultaneously, an intensified cold crystallization was observed, even in the PBS 30/PBAT 70 blend, where the thermal behavior without potato peels was predominantly governed by PBAT and showed no apparent cold crystallization. While the melting temperature remained stable in the range of 113–115 °C, an increase was also observed in melting enthalpy, by factors of 1.2, 1.3, and 32 for formulations PBS 70/PBAT 30, PBS 50/PBAT 50, and PBS 30/PBAT 70, respectively, each normalized to the total polymer content. This may indicate an increased degree of crystallinity in all potato peels-containing blends. However, the broadening of thermal transitions due to peak overlap between the two polymers could have again distorted the enthalpy values, particularly in blends with higher PBAT content.

In the polymer blends, only a single glass transition temperature was observed, which can be attributed to the close proximity of the T_g values of PBS and PBAT. A slight shift toward lower temperatures relative to the neat polymers was observed, with T_g values decreasing from −29.38 °C (PBS) and −25.85 °C (PBAT) to −28.78 °C, −31.11 °C and −32.71 °C in the 70/30, 50/
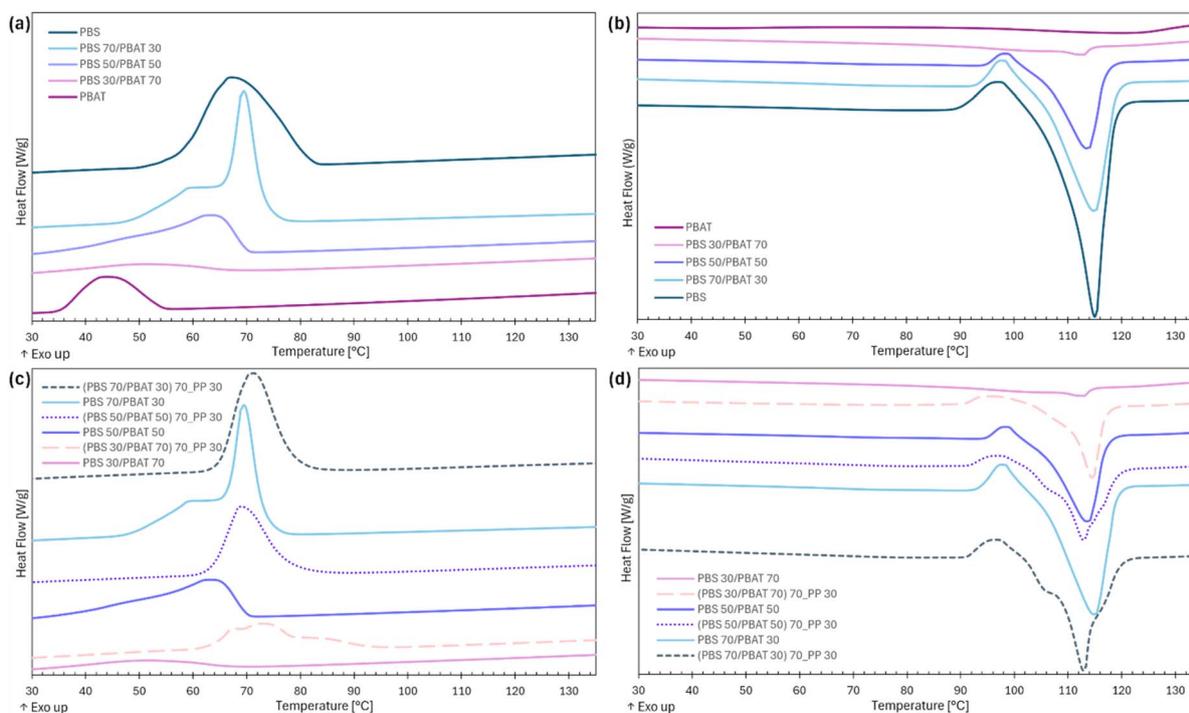

Fig. 4 DSC thermograms of PBS, PBAT, and PBS/PBAT blends showing (a) cooling and (b) second heating curves; and PBS/PBAT composites with 30 wt% potato peels (PP) showing (c) cooling and (d) second heating curves.

50 and 30/70 PBS/PBAT blends, respectively. Similar shifts have been reported in previous studies and may reflect underlying interchange reactions, potentially enhancing the compatibility between the two polymer phases,[9,46] as also suggested by the FTIR results. The glass transition temperature was further lowered upon incorporation of potato peels, indicating additional changes in interchain forces.[46]

3.3 Mechanical properties

The mechanical performance of the injection-molded specimens was evaluated based on their tensile and flexural properties. Particular attention was given to the effects of potato peels (PP) as a filler and their concentration, as well as to the polymer blend composition, on the elastic modulus, tensile strength, elongation at break, flexural modulus, and flexural strength (Table 3). Representative tensile stress–strain curves of all composite formulations are provided in Fig. S2–S4 (SI) to illustrate the deformation behavior. Incorporation of PP led to modifications in mechanical properties, notably a significant increase in the elastic modulus of both PBS- and PBAT-based compounds, in direct proportion to the filler concentration. Increases of 162% and 1418% were observed for PBS and PBAT composites containing 70 wt% PP, respectively, compared to their neat counterparts. This trend is consistent with previous findings, as natural fillers are known to reduce the ductility of polymer matrices by restricting chain mobility, thereby enhancing the stiffness of the resulting composite materials.[24,56,57] The reinforcing effect depends on the properties of

both the filler and the polymer matrix, the filler concentration, and its dispersion within the matrix.[56,58] PBS/PBAT blends exhibited elastic moduli intermediate to those of the neat polymers, with values decreasing as the proportion of PBAT increased. Similar behavior across a range of PBS/PBAT blend compositions has been reported in prior research, suggesting the presence of heterogeneous phase morphologies within the system.[5,14,21] Consistent with the results obtained for the neat polymers, the elastic moduli of the blends increased upon incorporation of 30 wt% PP, aligning between the corresponding PBS and PBAT composite values at the same filler content.

Concurrently with the increase in elastic moduli, the incorporation of PP resulted in significant reductions in both tensile strength and elongation at break. As suggested by FTIR analysis, the absence of strong interfacial interactions between the filler and the polymer matrices prevented any increase in tensile properties. Tensile strength decreased progressively from 35.0 MPa and 17.13 MPa for neat PBS and PBAT, respectively, to 10.61 MPa and 6.46 MPa at 70 wt% PP, corresponding to strength reductions of approximately 70% and 62%. These strength reductions may be attributed to the weak interfacial adhesion and limited compatibility between the hydrophobic polymer matrices and the hydrophilic PP, which impairs effective stress transfer within the biocomposites.[24,39,59,60] Moreover, non-uniform filler geometry[2] and the presence of voids or cavities within the composite structure[61] may have further compromised the mechanical integrity of the material. Polymer blending did not enhance the overall mechanical strength of the materials. While the tensile strength of the blends remained

Table 3 Elastic modulus, tensile strength and elongation at break of injection-molded dog bone specimens composed of PBS, PBAT and PBS/PBAT blends, as well as their corresponding composites containing 30–70% potato peels (PP). Values are presented as mean ± standard deviation ($n = 8$). Different superscript letters indicate statistically significant differences per property (column) between formulations within the same polymer matrix ($p \leq 0.05$)

Polymer matrix	Sample	Elastic modulus [MPa]	Tensile strength [MPa]	Elongation at break [%]	Flexural modulus [MPa]	Flexural strength [MPa]
PBS	PBS	697.9 ± 7.1 [A]	35.0 ± 1.2 [A]	251 ± 86 [A]	608 ± 22 [A]	21.34 ± 0.33 [A]
	PBS 70_PP 30	1171 ± 18 [B]	20.81 ± 0.31 [B]	3.81 ± 0.19 [B]	1126 ± 20 [B]	33.35 ± 0.13 [B]
	PBS 60_PP 40	1469 ± 19 [C]	18.13 ± 0.24 [C]	2.78 ± 0.16 [C]	1335 ± 54 [C]	34.81 ± 0.61 [C]
	PBS 50_PP 50	1532 ± 20 [D]	15.60 ± 0.24 [D]	2.20 ± 0.10 [D]	1466 ± 115 [D]	31.42 ± 0.79 [D]
	PBS 40_PP 60	1780 ± 43 [E]	12.18 ± 0.34 [E]	1.39 ± 0.17 [E]	1812 ± 39 [E]	25.66 ± 0.98 [E]
	PBS 30_PP 70	1825 ± 34 [E]	10.61 ± 0.31 [F]	0.92 ± 0.11 [F]	1952 ± 50 [F]	21.78 ± 0.96 [A]
PBAT	PBAT	76.5 ± 4.4 [A]	17.13 ± 0.79 [A]	299.20 ± 0.78 [A]	84.7 ± 4.8 [A]	2.92 ± 0.12 [A]
	PBAT 70_PP 30	283.0 ± 5.3 [B]	7.47 ± 0.19 [B]	89 ± 31 [B]	273.2 ± 7.8 [B]	8.55 ± 0.23 [B]
	PBAT 60_PP 40	453 ± 12 [C]	7.54 ± 0.33 [B]	11.9 ± 2.1 [C]	422 ± 12 [C]	11.31 ± 0.25 [C]
	PBAT 50_PP 50	614 ± 23 [D]	6.78 ± 0.31 [C]	6.8 ± 1.3 [D]	571 ± 21 [D]	12.33 ± 0.32 [D]
	PBAT 40_PP 60	865 ± 20 [E]	6.78 ± 0.23 [C]	3.51 ± 0.23 [E]	808 ± 20 [E]	13.14 ± 0.32 [E]
	PBAT 30_PP 70	1161 ± 42 [F]	6.46 ± 0.32 [C]	2.20 ± 0.64 [F]	1036 ± 34 [F]	11.42 ± 0.30 [C]
PBS/PBAT	PBS	697.9 ± 7.1 [A]	35.0 ± 1.2 [A]	251 ± 86 [A]	608 ± 22 [A]	21.34 ± 0.33 [A]
	PBAT	76.5 ± 4.4 [B]	17.13 ± 0.79 [CD]	299.20 ± 0.78 [A]	84.7 ± 4.8 [B]	2.92 ± 0.12 [B]
	PBS 70/PBAT 30	441 ± 22 [C]	24.6 ± 1.1 [B]	472 ± 80 [B]	446 ± 14 [C]	15.45 ± 0.42 [C]
	PBS 50/PBAT 50	338 ± 20 [D]	19.18 ± 0.90 [BC]	480 ± 49 [B]	340 ± 10 [D]	11.93 ± 0.47 [D]
	PBS 30/PBAT 70	222 ± 23 [E]	23.1 ± 6.6 [BC]	333 ± 58 [A]	227 ± 13 [E]	7.44 ± 0.53 [E]
	(PBS 70/PBAT 30) 70_PP 30	873 ± 21 [F]	15.62 ± 0.23 [DE]	4.78 ± 0.26 [D]	840 ± 27 [F]	24.51 ± 0.42 [F]
	(PBS 50/PBAT 50) 70_PP 30	678 ± 14 [G]	12.96 ± 0.24 [EF]	7.3 ± 1.1 [CD]	652 ± 17 [G]	19.23 ± 0.42 [G]
	(PBS 30/PBAT 70) 70_PP 30	461 ± 20 [C]	10.05 ± 0.31 [F]	12.7 ± 2.3 [C]	461 ± 23 [C]	14.01 ± 0.40 [H]

within the bounds set by the neat polymers, the incorporation of PP similarly led to a significant reduction in tensile performance.

The altered structure and reduced ductility resulting from potato peel incorporation also led to a significant decrease in elongation at break. A substantial decline was already evident at 30 wt% filler loading, with 70 wt% resulting in reductions from 251 to 0.92% for PBS and from 299.20 to 2.20% for PBAT, respectively.

While blending PBS and PBAT has previously been associated with reduced ductility in filler-free systems,[14,21] the present study observed a 1.8-fold increase in elongation at break, suggesting enhanced interactions between the two polymer phases. Previous research has shown that blending these inherently immiscible polymers resulted in the formation of a two-phase morphology, either as a droplet-matrix structure or a co-continuous phase morphology.[5,9,14,21,62] The absence of a distinct interface between the phases has been attributed to interactions and partial compatibility between the two polymers,[14] which have been linked to increased complex viscosity and storage modulus[5,9,21] as well as enhanced elastic response.[5,43] In the present study, possible interactions between the polymer phases were also suggested by FTIR analysis, particularly in the PBS 70/PBAT 30 blend. However, the morphological structure formed has been reported to be strongly influenced by the blend ratio, processing temperature, and shear rate.[62] In this study, a slight decrease in elongation at break was observed at 70 wt% PBAT content. However, the incorporation of PP into the blends caused a similarly pronounced decrease in ductility as observed in the neat polymers. Overall, the extent of compatibilization appeared to be limited[5,9,21] and, consequently, may have been insufficient to compensate for the weakening effect of filler addition.

In general, the effects of incorporating potato peels into PBS, PBAT, and their blends were comparable to those reported for their use as a filler in other polymer matrices. Similar trends, namely, reductions in tensile strength and elongation at break, along with an increase in elastic modulus, have also been observed in composites based on polypropylene, linear low-density polyethylene (LLDPE), and polylactic acid (PLA), resulting in a corresponding reduction in matrix ductility and an overall enhancement in stiffness.[38–40] While the incorporation of PP into PBS/PBAT blends also induced pronounced alterations in material behavior, the resulting composites exhibited more balanced mechanical properties compared to the individual polymer-based systems.

In parallel with the increase in elastic modulus, the flexural modulus was likewise enhanced upon incorporation of PP. This stiffening effect was consistently observed across both the individual polymers and their blends, indicating the reinforcing role of the filler. Consistent with Sugumaran et al. (2015), no material failures occurred at lower PP contents of up to 40 wt%, resulting in greater flexural deformation and increased flexural strength compared to the neat polymers and their blends.[38] The quality of the interface between the polymer matrix and the filler was shown to have a less pronounced effect on flexural performance than on tensile properties.[56] At higher PP

concentrations, however, fracture occurred, accompanied by a decrease in flexural strength.

3.4 Surface wettability and water absorption behavior

Surface characteristics and water sensitivity of PBS, PBAT, and their blends were evaluated in relation to 30–70% potato peel content by measuring the water contact angle (WCA), water uptake capacity (WUC), and soluble matter loss (SML) (Table 4). In PBS, a gradual decrease in WCA was observed with increasing PP content, from 87.4° in neat PBS to 72.2° at 70% loading. Natural fillers are known to exhibit a hydrophilic nature due to their composition, which includes a high density of polar functional groups such as hydroxyl and carboxyl groups, commonly present in starch, cellulose, and hemicellulose.[25,50,63] In addition, poor interfacial adhesion and limited compatibility between PBS and PP, as already reflected in the mechanical performance, may lead to matrix disruption by the filler particles, promoting crack formation and the development of interfacial microvoids, which in turn can facilitate water uptake.[25,64,65] These effects were further supported by the increased water absorption and soluble matter loss observed in PBS composites with higher filler contents. While the water uptake of the neat polymer was found to be negligible (0.43 ± 0.05%), WUC values of up to 10.56% were measured in composites containing 70% PP.

In contrast, a significant increase in water contact angle was observed for both PBAT and the PBS/PBAT blends, occurring at 30–40% and 30% PP content, respectively. The complex composition of PP, along with varying interactions between the filler and different polymer matrices, may contribute to the observed differences in surface properties. Miller et al. (2024) reported that injection-molded PLA samples containing 10% PP exhibited a polymer-dominated surface characterized by a smooth layer free of PP constituents.[40] Conversely, the incorporation of lignin[66] and polyphenols[67] into PBAT-based composites has been associated with increased WCA values. Several components of PP, such as proteins, lignin/suberin, and lipids, may contribute to more hydrophobic surface characteristics due to their intrinsic hydrophobicity.[25] If these components migrate to, or agglomerate at, the surface, they may reduce the overall surface polarity of the composite. Additionally, surface roughness is known to amplify a material's intrinsic wettability, thereby potentially influencing the water contact angle.[68] Thus, an increase in hydrophobicity indicated by higher contact angles may reflect surface effects rather than a fundamental reduction in water sensitivity. This is supported by WUC values, which showed that water absorption still significantly increased with filler addition in PBAT and blend composites, from 0.53% to 12.42% at 70% loading in PBAT, and from 0.36–0.43% to 1.96–2.08% at 30% PP in the blends.

The degree of crystallinity is known to influence the water absorption behavior of polymers. The larger proportion of amorphous regions in PBAT makes it more accessible to water uptake compared to PBS, which exhibits a higher degree of crystallinity.[30] This structural factor aligns with the observed

Table 4 Water contact angle (WCA), water uptake capacity (WUC) and soluble matter loss (SML) of injection-molded dog bone specimens composed of PBS, PBAT and PBS/PBAT blends, as well as their corresponding composites containing 30–70% potato peels (PP). Values are presented as mean ± standard deviation ($n = 5$). Different superscript letters indicate statistically significant differences between formulations within the same polymer matrix ($p \leq 0.05$)

Polymer matrix	Sample	WCA [°]	WUC [%]	SML [%]
PBS	PBS	87.4 ± 2.6 [A]	0.43 ± 0.05 [A]	0.03 ± 0.01 [A]
	PBS 70_PP 30	78.5 ± 2.6 [A]	1.99 ± 0.04 [B]	0.35 ± 0.04 [B]
	PBS 60_PP 40	74.0 ± 2.2 [B]	2.88 ± 0.05 [C]	0.33 ± 0.03 [B]
	PBS 50_PP 50	72.8 ± 2.2 [B]	4.34 ± 0.10 [D]	0.54 ± 0.05 [C]
	PBS 40_PP 60	74.3 ± 1.5 [B]	7.37 ± 0.25 [E]	1.00 ± 0.07 [D]
	PBS 30_PP 70	72.2 ± 1.9 [B]	10.56 ± 0.24 [F]	1.58 ± 0.12 [E]
PBAT	PBAT	87.7 ± 1.7 [AB]	0.53 ± 0.01 [A]	0.04 ± 0.01 [A]
	PBAT 70_PP 30	94.4 ± 1.9 [C]	2.43 ± 0.02 [B]	0.11 ± 0.02 [B]
	PBAT 60_PP 40	92.1 ± 1.9 [C]	3.55 ± 0.22 [C]	0.22 ± 0.09 [B]
	PBAT 50_PP 50	88.8 ± 2.4 [B]	5.39 ± 0.15 [D]	0.39 ± 0.04 [C]
	PBAT 40_PP 60	83.7 ± 5.8 [A]	7.42 ± 0.25 [E]	0.56 ± 0.09 [C]
	PBAT 30_PP 70	83.7 ± 3.4 [A]	12.42 ± 0.51 [F]	1.33 ± 0.16 [D]
PBS/PBAT	PBS	87.4 ± 2.6 [A]	0.43 ± 0.05 [B]	0.03 ± 0.01 [C]
	PBAT	87.7 ± 1.7 [A]	0.53 ± 0.01 [CD]	0.04 ± 0.01 [C]
	PBS 70/PBAT 30	75.1 ± 3.0 [B]	0.39 ± 0.01 [AB]	0.00 ± 0.01 [A]
	PBS 50/PBAT 50	75.8 ± 4.5 [B]	0.36 ± 0.01 [A]	0.00 ± 0.00 [A]
	PBS 30/PBAT 70	86.4 ± 1.8 [A]	0.43 ± 0.01 [BC]	0.01 ± 0.00 [B]
	(PBS 70/PBAT 30) 70_PP 30	96.1 ± 1.5 [C]	1.96 ± 0.06 [DE]	0.19 ± 0.03 [E]
	(PBS 50/PBAT 50) 70_PP 30	96.2 ± 1.3 [C]	2.04 ± 0.04 [E]	0.15 ± 0.01 [E]
	(PBS 30/PBAT 70) 70_PP 30	96.2 ± 1.2 [C]	2.08 ± 0.07 [E]	0.13 ± 0.01 [D]

trend, in which PBS consistently exhibited slightly lower water uptake than PBAT.

Overall, although wettability and water absorption are important factors in the biodegradability of biocomposites,[65] an increase in these properties associated with higher filler content negatively affects material performance and limits the applicability of the materials.[24] Therefore, water sensitivity remains a critical parameter in the optimization of biocomposite formulations.

Conclusions

This study demonstrates that potato peel powder, an abundant and underutilized agricultural by-product, can be effectively employed as a reinforcing filler in PBS, PBAT, and PBS/PBAT blend-based biocomposites. The successful incorporation of high filler contents of up to 70 wt% *via* injection molding not only validates the processability of these systems but also represents a promising approach to reducing fossil-based polymer content. The observed increases in stiffness and the ability to tailor mechanical performance through polymer blending highlight the potential of these formulations for application-specific development in the bio-based materials sector.

A key contribution of this study lies in deepening the understanding of interfacial behavior in biocomposites comprising hydrophilic lignocellulosic fillers and hydrophobic biodegradable polymer matrices. The pronounced reductions in ductility and moisture resistance observed at higher filler loadings reflect interfacial incompatibility, a known limitation in such heterogeneous systems. However, the inherent partial miscibility between PBS and PBAT, combined with their compositional tunability, offers a promising framework for optimizing phase morphology, interfacial adhesion, and overall composite performance through targeted formulation and reactive processing strategies. Thermal analysis further revealed that potato peels act as heterogeneous nucleating agents, particularly enhancing crystallization in PBS and PBS-rich blends. However, the overall degree of crystallinity was only moderately affected overall, with non-linear trends suggesting a balance between nucleation promotion and chain mobility restriction.

Future research should focus on the development of compatibilization strategies, including the use of reactive additives, surface functionalization of the filler, or compatibilizer polymers, to enhance interfacial bonding and reduce water uptake. Moreover, further investigations into thermal stability, barrier properties, long-term performance, and biodegradability under realistic conditions will be essential for evaluating the full application potential of these materials in packaging, agriculture, or low-load consumer goods.

Overall, the findings contribute to the advancement of circular bioeconomy approaches by demonstrating how food processing by-products can be converted into value-added composite materials that combine reduced environmental impact with functional performance.

Author contributions

Susanna Miescher: conceptualization, methodology, investigation, visualization, project administration, writing – original draft and review. Florine Schleiffer: methodology, investigation. Eliane Wegenstein: investigation. Selçuk Yildirim:

conceptualization, writing – review & editing, supervision, funding acquisition.

Conflicts of interest

The authors declare no conflict of interest.

Data availability

The data supporting this article have been included within the article and additionally as part of the supplementary information (SI). Supplementary information is available. See DOI: https://doi.org/10.1039/d5fb00333d.

Acknowledgements

References

1 J. Stanley, D. Culliton, A.-J. Jovani-Sancho and A. C. Neves, *Eng*, 2025, **6**, 17.

2 D. C. McNeill, A. K. Pal, A. K. Mohanty and M. Misra, *Compos., Part C: Open Access*, 2023, **12**, 100388.

3 M. Lackner, A. Mukherjee and M. Koller, *Polymers*, 2023, **15**, 4695.

4 S. Pathak, C. Sneha and B. B. Mathew, *J. Polym. Biopolym. Phys. Chem.*, 2014, **2**, 84–90.

5 E. Pesaranhajiabbas, A. K. Pal, A. Rodriguez-Uribe, A. K. Mohanty and M. Misra, *ACS Appl. Polym. Mater.*, 2022, **4**, 5546–5556.

6 F. Wu, M. Misra and A. K. Mohanty, *RSC Adv.*, 2019, **9**, 2836–2847.

7 M. Barletta, C. Aversa, M. Ayyoob, A. Gisario, K. Hamad, M. Mehrpouya and H. Vahabi, *Prog. Polym. Sci.*, 2022, **132**, 101579.

8 M. Okada, *Prog. Polym. Sci.*, 2002, **27**, 87–133.

9 R. Muthuraj, M. Misra and A. K. Mohanty, *J. Polym. Environ.*, 2014, **22**, 336–349.

10 E. Sasimowski, Ł. Majewski and M. Grochowicz, *Materials*, 2021, **14**, 7049.

11 M. Barletta, A. Genovesi, M. P. Desole and A. Gisario, *Clean Technol. Environ. Policy*, 2024, **27**, 683–725.

12 S. A. Rafiqah, A. Khalina, A. S. Harmaen, I. A. Tawakkal, K. Zaman, M. Asim, M. N. Nurrazi and C. H. Lee, *Polymers*, 2021, **13**, 1436.

13 V. Rajgond, A. Mohite, N. More and A. More, *Polym. Bull.*, 2024, **81**, 5703–5752.

14 A. R. de Matos Costa, A. Crocitti, L. Hecker de Carvalho, S. C. Carroccio, P. Cerruti and G. Santagata, *Polymers*, 2020, **12**, 2317.

15 J. Xu and B.-H. Guo, *Biotechnol. J.*, 2010, **5**, 1149–1163.

16 F. V. Ferreira, L. S. Cividanes, R. F. Gouveia and L. M. F. Lona, *Polym. Eng. Sci.*, 2019, **59**, E7–E15.

17 A. K. Maurya, F. M. de Souza, T. Dawsey and R. K. Gupta, *Polym. Compos.*, 2024, **45**, 2896–2918.

18 N. d. C. L. Beluci, J. d. Santos, F. A. de Carvalho and F. Yamashita, *Carbohydr. Polym. Technol. Appl.*, 2023, **5**, 100274.

19 Y. Li, C. Li, H. Ma, R. Gong, G. Mu, Y. Wang, L. Ren and M. Zhang, *J. Polym. Res.*, 2025, **32**, 137.

20 B. E. Itabana, A. K. Mohanty, P. Dick, M. Sain, A. Bali, M. Tiessen, L.-T. Lim and M. Misra, *Macromol. Mater. Eng.*, 2024, **309**, 2400179.

21 A. Boonprasertpoh, D. Pentrakoon and J. Junkasem, *J. Met., Mater. Miner.*, 2017, **27**(1), 1–11.

22 S.-F. Yao, X.-T. Chen and H.-M. Ye, *J. Phys. Chem. B*, 2017, **121**, 9476–9485.

23 A. Mtibe, L. Hlekelele, P. E. Kleyi, S. Muniyasamy, N. E. Nomadolo, O. Ofosu, V. Ojijo and M. J. John, *Polymers*, 2022, **14**, 5065.

24 D. C. McNeill, A. K. Pal, A. K. Mohanty and M. Misra, *J. Appl. Polym. Sci.*, 2024, **141**, e55166.

25 L. Wei, S. Liang and A. G. McDonald, *Ind. Crops Prod.*, 2015, **69**, 91–103.

26 R. Muthuraj, M. Misra and A. K. Mohanty, *AIP Conf. Proc.*, 2015, 1664.

27 Y. N. Hamou, S. Benali, M. Benomar, S. Gennen, J.-M. Thomassin, J. Tchoumtchoua, H. Er-Raioui and J.-M. Raquez, *J. Appl. Polym. Sci.*, 2025, **142**, e56959.

28 N. Bumbudsanpharoke, P. Wongphan, K. Promhuad, P. Leelaphiwat and N. Harnkarnsujarit, *Food Control*, 2022, **132**, 108541.

29 H. S. M. Lopes, G. H. M. de Oliveira, T. H. S. Maia, C. G. Renda and A. de Almeida Lucas, *Iran. Polym. J.*, 2023, **32**, 313–324.

30 S. Y. Yap, S. Sreekantan, M. Hassan, K. Sudesh and M. T. Ong, *Polymers*, 2021, **13**, 104.

31 Z. C. Lule, E. Wondu and J. Kim, *J. Cleaner Prod.*, 2021, **315**, 128095.

32 FAO, Crops and livestock products, https://www.fao.org/faostat/en/#data, accessed February 26, 2024, 2024.

33 A. Chauhan, F. Islam, A. Imran, A. Ikram, T. Zahoor, S. Khurshid and M. A. Shah, *Food Sci. Nutr.*, 2023, **11**, 5773–5785.

34 K. Rommi, J. Rahikainen, J. Vartiainen, U. Holopainen, P. Lahtinen, K. Honkapää and R. Lantto, *J. Appl. Polym. Sci.*, 2016, **133**(5), 1–11.

35 M. E. Camire, D. Violette, M. P. Dougherty and M. A. McLaughlin, *J. Agric. Food Chem.*, 1997, **45**, 1404–1408.

36 S. Liang and A. G. McDonald, *J. Agric. Food Chem.*, 2014, **62**, 8421–8429.

37 S. Miescher, L. Hülsmann and S. Yildirim, *Packag. Technol. Sci.*, 2024, **37**, 929–939.

38 V. Sugumaran, K. K. Vimal, G. S. Kapur and A. K. Narula, *J. Appl. Polym. Sci.*, 2015, **132**(34), 1–9.

39 V. Sugumaran, G. S. Kapur and A. K. Narula, *Polym. Bull.*, 2018, **75**, 5513–5533.

40 K. Miller, C. L. Reichert, M. Loeffler and M. Schmid, *Compounds*, 2024, **4**, 119–140.

41 A. Gowman, T. Wang, A. Rodriguez-Uribe, A. K. Mohanty and M. Misra, *ACS Omega*, 2018, **3**, 15205–15216.

42 T. Miyata and T. Masuko, *Polymer*, 1998, **39**, 1399–1404.

43 P. C. G. Conceição, P. V. F. Lemos, J. S. Santana, P. R. C. Correia, L. G. Cardoso, D. de Jesus Assis, L. P. G. da Rocha, H. R. Marcelino, E. de Souza Ferreira, J. B. A. da Silva and C. O. de Souza, *J. Appl. Polym. Sci.*, 2024, **141**, e55289.

44 Q. Yin, F. Chen, H. Zhang and C. Liu, *Plast., Rubber Compos.*, 2015, **44**, 362–367.

45 C.-H. Tsou, Z.-J. Chen, S. Yuan, Z.-L. Ma, C.-S. Wu, T. Yang, C.-F. Jia and M. Reyes De Guzman, *Curr. Res. Green Sustainable Chem.*, 2022, **5**, 100329.

46 J. John, R. Mani and M. Bhattacharya, *J. Polym. Sci., Part A: Polym. Chem.*, 2002, **40**, 2003–2014.

47 B. Shrestha, S. Shah, K. Chapain, R. Joshi and R. Pandit, *Spectr. Emerg. Sci.*, 2022, **2**, 45–52.

48 Q. Mushtaq, N. Joly, P. Martin and J. I. Qazi, *Molecules*, 2023, **28**, 7250.

49 Y. Xie, X. Niu, J. Yang, R. Fan, J. Shi, N. Ullah, X. Feng and L. Chen, *Int. J. Biol. Macromol.*, 2020, **150**, 480–491.

50 X. Zhai, J. Han, L. Chang, F. Zhao, R. Zhang, W. Wang and H. Hou, *Int. J. Biol. Macromol.*, 2024, **277**, 134505.

51 M. Sadeghi-Shapourabadi, M. Robert and S. Elkoun, *Appl. Sci.*, 2025, **15**, 6385.

52 S. Radhakrishnan, S. Thorat, A. Desale, P. Desai and M. B. Kulkarni, *IOP Conf. Ser.:Mater. Sci. Eng.*, 2022, **1248**, 012013.

53 O. Platnieks, S. Gaidukovs, A. Barkane, G. Gaidukova, L. Grase, V. K. Thakur, I. Filipova, V. Fridrihsone, M. Skute and M. Laka, *Molecules*, 2020, **25**, 121.

54 W. Pivsa-Art, K. Fujii, K. Nomura, Y. Aso, H. Ohara and H. Yamane, *J. Polym. Res.*, 2016, **23**, 144.

55 M. R. Nobile, A. Crocitti, M. Malinconico, G. Santagata and P. Cerruti, *AIP Conf. Proc.*, 2018, 1981.

56 H. Oliver-Ortega, M. F. Llop, F. X. Espinach, Q. Tarrés, M. Ardanuy and P. Mutjé, *Composites, Part B*, 2018, **152**, 126–132.

57 V. Guna, M. Ilangovan, M. H. Rather, B. V. Giridharan, B. Prajwal, K. Vamshi Krishna, K. Venkatesh and N. Reddy, *J. Build. Eng.*, 2020, **27**, 100991.

58 F. Wu, M. Misra and A. K. Mohanty, *Compos. Sci. Technol.*, 2020, **200**, 108369.

59 H.-S. Kim and H.-J. Kim, *Fibers Polym.*, 2013, **14**, 793–803.

60 J. Li, X. Luo, X. Lin and Y. Zhou, *Starch - Stärke*, 2013, **65**, 831–839.

61 Y. J. Phua, W. S. Chow and Z. A. Mohd Ishak, *Polym. Degrad. Stab.*, 2011, **96**, 1194–1203.

62 J. Yin, Q.-F. Ouyang, Z.-B. Sun, F.-Y. Wu, Q. Liu, X.-X. Zhang, L. Xu, H. Lin, G.-J. Zhong and Z.-M. Li, *Chin. J. Polym. Sci.*, 2022, **40**, 593–601.

63 J.-B. Zeng, L. Jiao, Y.-D. Li, M. Srinivasan, T. Li and Y.-Z. Wang, *Carbohydr. Polym.*, 2011, **83**, 762–768.

64 C. Gozdecki and A. Wilczyn, *Wood Fiber Sci.*, 2015, **47**, 365–374.

65 A. K. Zykova, P. V. Pantyukhov, N. N. Kolesnikova, T. V. Monakhova and A. A. Popov, *J. Polym. Environ.*, 2018, **26**, 1343–1354.

66 M. Li, Y. Jia, X. Shen, T. Shen, Z. Tan, W. Zhuang, G. Zhao, C. Zhu and H. Ying, *Ind. Crops Prod.*, 2021, **171**, 113916.

67 Z. Zhang, Y. Wang, X. Fang, X. Chen, Z. Yin and C. Zhang, *Front. Sustain. Food Syst.*, 2024, **8**, 1470732.

68 M. Soccio, F. Dominici, S. Quattrosoldi, F. Luzi, A. Munari, L. Torre, N. Lotti and D. Puglia, *Biomacromolecules*, 2020, **21**, 3254–3269.